

Methods

Biochemistry on PSD fraction. The cerebral cortices for PSD fractionation were dissected out and cut into slices (0.25 mm) with a McIlwain tissue chopper. The slices were pre-incubated for 30 min at 37°C in 10 ml of oxygenated Krebs-HEPES buffer (KHB) containing 25 mM HEPES-sodium salt, 100 mM NaCl, 5 mM KCl, 1.2 mM MgCl₂, 2.5 mM CaCl₂, 10 mM, glucose, pH 7.4. The KHB was kept oxygenated and at 37°C at all times. Slices were washed three times with KHB (twenty slices per tube) before incubation for 1 hr in KHB containing either 100 μM Picotoxin, 10 mM MgCl₂, or 1 μM TTX.

PSDs were purified from cortex slices or in some cases directly from brains of adult rats as described previously (Huang et al., 2000). In brief, tissues were homogenized in buffered sucrose (0.32 M sucrose and 4 mM HEPES/NaOH, pH 7.4) with a glass-Teflon homogenizer. The homogenate was centrifuged at 800 X g for 10 min. The supernatant (S1) was centrifuged at 9000 X g for 15min, yielding P2 (the crude synaptosomal fraction) and S2. The P2 fraction was resuspended in the homogenizing buffer and subjected to another centrifugation at 10,000 X g for 15 min. The resulting pellet was lysed by hypo-osmotic shock in water, rapidly adjusted to pH 7.4 with 1 mM HEPES/NaOH, and stirred on ice for 30 min. The resuspended pellet was then centrifuged at 25,000 X g for 20 min, yielding the P3 fraction. The P3 fraction was resuspended in 0.25 M buffered sucrose, layered onto a discontinuous sucrose gradient containing 0.8/1.0/1.2 M sucrose, and centrifuged for 2 hr at 65,000 X g. The gradient yielded a synaptosomal plasma membrane (SPM) fraction at the 1.0/1.2 M sucrose

interface. The SPM fraction was solubilized with 0.4% Triton X-100 in 0.5mM HEPES/NaOH, pH 7.4, and subjected to centrifugation at 25,000 X g for 20 min, yielding an insoluble PSD fraction.

Immunoprecipitation and Western Blotting. Immunoprecipitation was carried out as previously described (Huang et al., 2000). Briefly, The brain homogenate or PSD fraction (~500 µg of protein) were incubated with indicated antibodies (1-2 µg) at 4°C for 1 hr with constant rocking in 1 ml of the modified RIPA buffer (50 mM Tris-HCl, pH 7.4, 150 mM NaCl, 1% NP-40, 0.25% sodium-deoxycholate, 1 mM PMSF, 1 mM EDTA, 1 µg/ml Aprotinin, leupeptin, and pepstatin protease inhibitors). Protein A- agarose beads (50 µl) were added and incubated at 4 °C for 1 hr. After washing, bound proteins were resolved by SDS-PAGE and transferred onto a nitrocellulose membrane (Whatman Inc). Membranes were blocked with PBS containing 5% non-fat dry milk and 0.05% Tween 20 for 1 hr, and incubated overnight at 4°C with primary antibodies, followed by incubation with horseradish peroxidase-conjugated secondary antibody (Amersham Pharmacia). Immunoreactivity was visualized by autoradiogram using an enhanced chemiluminescence system (Amersham Pharmacia).

Antibodies used were from Upstate Technology (anti PSD-95), Santa Cruz (anti ErbB4) and Transduction Labs (anti phosphotyrosine).

Electrophysiology. Whole-cell recordings were obtained with Axopatch-1D amplifiers (Molecular Devices, Foster City, CA). To monitor the effects of different constructs on synaptic transmission, slices were either transfected biolistically or infected with Sindbis or Lenti viruses expressing different constructs. Two days (biolistic), 16 – 24 h (Sindbis virus), or 4 – 7 days (Lenti virus) later, whole-cell recordings were obtained simultaneously from a transfected and an adjacent nontransfected neuron in the CA1 region under visual guidance using epifluorescence and transmitted light illumination. The recording chamber was perfused with artificial cerebrospinal fluid (ACSF) containing 119 mM NaCl, 2.5 mM KCl, 4 mM CaCl₂, 4 mM MgCl₂, 26 mM NaHCO₃, 1 mM NaH₂PO₄, 11 mM Glucose, 0.1 mM picrotoxin, and 1 μM 2-chloroadenosine (pH 7.4) and gassed with 5% CO₂/95% O₂. Recordings were made at 27°C. Patch recording pipettes (3-5 MΩ) were filled with intracellular solution containing 115 mM cesium methanesulfonate, 20 mM CsCl, 10 mM HEPES, 2.5 mM MgCl₂, 4 mM Na₂ATP, 0.4 mM Na₃GTP, 10 mM sodium phosphocreatine, and 0.6 mM EGTA (pH 7.25). Evoked responses were induced using bipolar electrodes placed on Schaffer collateral pathway or CA3 cell body regions. Responses were recorded at both –60 (for AMPA receptor mediated responses) and +40 (for NMDA receptor mediated responses) mV. NMDA receptor mediated responses were quantified as the mean between 110-160 ms after stimulation. Conventional LTP was induced by pairing postsynaptic depolarization at 0 mV with presynaptic stimulation at 3 Hz for 1.5 min. Approximately one-half of experiments were done and analyzed blind with respect to construct expressed. Results were similar and thus pooled with non-blind results. Statistical significance was determined by Student's t test or Kolmogorov–Smirnov test. Spontaneous responses

(mEPSCs) were recorded at 27 °C in the presence of 1 μ M TTX and 0.1 mM picrotoxin and analyzed using Mini Analysis Program (Synaptosoft).

Two-photon laser-scanning microscopy and cLTP induction. Experiments were performed at 30°C in physiological artificial CSF (ACSF) (in mM: 119 NaCl, 26 NaHCO₃, 1 NaH₂PO₄, 11 D-glucose, 2.5 KCl, 4 CaCl₂, 4 MgCl₂, and 1.25 NaHPO₄) gassed with 5% CO₂ and 95% O₂. The cLTP induction solution consisted of the above ACSF lacking MgCl₂ and containing 100 nM Rolipram, 50 μ M forskolin, and 100 μ M picrotoxin (all dissolved in DMSO at 1000x). Before TPLSM imaging, transfected CA1 pyramidal neurons were identified by epifluorescence illumination. High-resolution three-dimensional image stacks were collected on a custom-built instrument based on a Fluoview laser-scanning microscope (Olympus America, Melville, NY). The light source was a mode-locked Ti:sapphire laser (Mira 900F; Mira, Santa Clara, CA) running at 910 nm. We used an Olympus 60x 1.1 numerical aperture objective. Each optical section was resampled three times and was captured every 0.5 μ m. For experiments to compare spine size and density, sister cultures were always used to transfect or infect with different constructs for comparison. Images were taken from regions on apical dendrites, which were typically about 100 μ m away from the soma and covered 150-200 μ m in length. For cLTP experiments, a standard region encompassing the initial bifurcation of the CA1 neuron was chosen for data acquisition. Two full stacks were captured (at -30 and -10 min) before cLTP induction. One stack was captured during the 16 min induction at +5 min and two after induction at +40 and +70 min. During the cLTP induction, 10 ml of the induction solution was allowed to flow through before recycling to prevent mixing of the

solutions. After the 16 min induction, 10 ml of the basal solution was allowed to flow through before recycling.

Image display. All images displayed in the manuscript are data from consecutive stacks displayed using a maximum value projection. At any given x - y coordinate, the maximum pixel value in that Z -column is displayed in the two-dimensional image. Ratio images are displayed for two-channel data (green/red; i.e., receptor/volume) and mapped in pseudocolor with red representing a high ratio and blue a low ratio. Image analysis was conducted on raw data using full Z -stacks as discussed below.

Quantitative image analysis. The image data was analyzed as previously described (Kopec et al., 2006). Briefly, spines were analyzed using custom software written in MatLab. All analyses were conducted blind to the receptor being expressed. For each experiment, projection images of 40–60 consecutive z -series sections were generated for each cell or each time point. Spines were identified using the tDimer or tomato dsRed channel, and rectangular regions of interest (ROIs) were manually positioned to fully cover each spine. For cLTP experiments, all spines identified in the first time point were followed for all of the subsequent time images, and thus the choice was blind with respect to the outcome. Individual spines were numbered and followed in a time-lapse recording. When the identity of a protrusion was unclear (for instance, two spines appear as one), the specific spine was not included in the analysis. In addition, no effort was made to analyze spines emerging below or above the dendrite, because the TPLSM resolution of these is compromised. It is also possible that many small structures were not detected, although point spread function-limited structures were observed. Dendrite ROIs were placed at the

base of each spine centered on the dendrite with approximately the same area as the corresponding spine ROI. Total integrated fluorescence (in arbitrary units) for both green and red channels were computed for each section in a stack. Background and spillover (from the other channel) fluorescence were subtracted to generate a background- and spillover-subtracted integrated fluorescence value for each channel as a function of depth. Z-boundaries were defined by the full-width at half-maximum of the tDimer or tomato dsRed channel (X and Y boundaries defined by the ROI). Red and green fluorescence was then integrated within these boundaries. For dendrite ROIs, the mean pixel fluorescence (rather than integrated fluorescence) was taken within these boundaries to negate any effect that alterations in the size of the ROI would have. The integrated red fluorescence (from tDimer or tomato dsRed) value was used as a measurement of spine volume. In order to compare spine size for different neurons, the spine integrated red fluorescence was normalized to the mean red fluorescence value measured in the soma for each cell to normalize the expression levels of the red mark proteins. The values were then normalized to the spine size of the control group to allow for comparison between different experiments. Only pixels that were >3 SDs above background were included in the average. Significance was determined by *t* test of data after cLTP induction versus baseline.

Enrichment of receptors on spines is defined as $(\text{spine green}/\text{spine red fluorescence})/(\text{dendrite green}/\text{dendrite red fluorescence})$. This technique is used as a relative not absolute means of determining enrichment. Data from each group were plotted as a cumulative distribution; significant differences were determined by a Kolmogorov–Smirnov test.

Neuronal culture and Western blotting: dissociated neuronal cultures were made from embryonic day 18 rats as described previously (Li et al., 2003). SDS-PAGE and Western blotting were used to determine the expression levels of erbB4 and NRG1 as described previously (Huang et al., 2000; Wang et al., 2001). The antibodies used were sc-283 (erbB4) and sc-348 (NRG1) from Santa Cruz Biotechnology.

HEK293 cell transfection and imaging: HEK293 cells were transfected using Lipofectamine 2000 (Invitrogen). About 24 to 36 hours after transfection cells were imaged with TPLSM to examine protein expression.

Supplemental Figure 1. erbB4 RNAi suppresses the expression of erbB4. A.

Dissociated rat hippocampal neuronal cultures were infected with Lenti virus expressing GFP only, un-infected, or infected with Lenti virus expressing GFP together with short hairpin RNAs targeting erbB4 (hp1, hp2, or hp3). Upper bands: Protein samples resolved by SDS PAGE and stained with anti-erbB4 antibody. Hp2 most efficiently suppressed erbB4 expression. Lower bands: the same blot was stripped and stained with anti-tubulin antibody to serve as loading control. B. Quantification of the EPSCs recorded from paired un-infected (control) and infected (hp1, hp2, or hp3) CA1 cells from cultured hippocampal slices. Hp2 and hp3 effectively suppressed synaptic transmission (AMPA: hp2 0.59 ± 0.08 over control, n= 4 pairs, $P < 0.05$; hp3 0.55 ± 0.06 , n=7 pairs, $P < 0.05$; NMDAR: hp2 0.58 ± 0.1 over control, n= 4 pairs, $P = 0.05$; hp3 0.6 ± 0.14 , n=7 pairs, $P = 0.05$), whereas hp1 was not effective (AMPA: hp1 0.77 ± 0.11 over control, n= 6 pairs, $P > 0.05$; NMDAR: hp1 0.87 ± 0.07 over control, n=5 pairs, $P > 0.05$). C.

Quantification of the EPSCs recorded from paired un-infected (control) and infected

cells. Cells were infected with a lenti virus expressing erbB4 hp2 together with an erbB4 construct with silent mutations that avoid targeting by hp2. The effects on synaptic transmission were similar to expressing erbB4 alone. (AMPA: control 1 ± 0.27 ; infected: 1.6 ± 0.36 , $n=7$ pairs, $P < 0.01$; NMDAR: control 1 ± 0.22 ; infected 1.2 ± 0.27 , $n=7$ pairs, $P > 0.05$).

Supplemental Figure 2. NRG1 RNAi suppresses the expression of NRG1 isoforms.

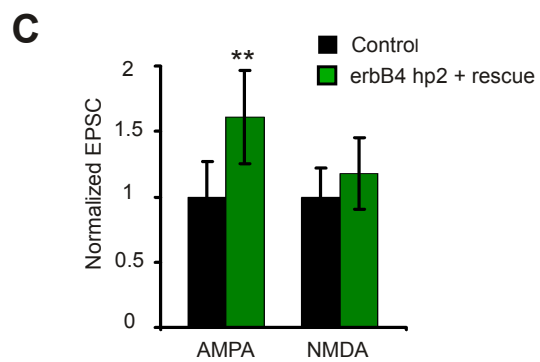
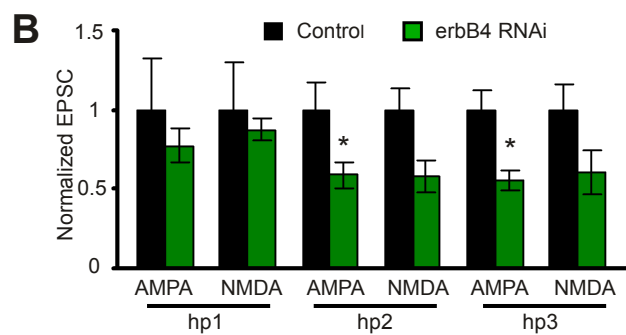
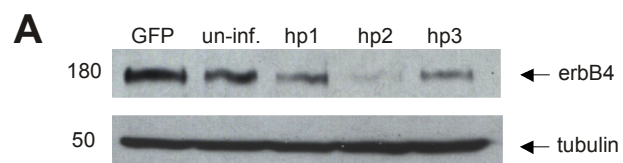
A. Dissociated rat hippocampal neuronal cultures were infected with Lenti virus expressing GFP only, uninfected, or infected with Lenti virus expressing GFP together with short hairpin RNAs targeting NRG1 (hp1, hp2, or hp3). Upper bands: Protein samples resolved by SDS PAGE and stained with anti-NRG1 antibody. The 140 kDa band represents NRG1 type III, whereas the 110 kDa band could be from both NRG1 type I and type III (Wang et al., 2001). Left: the shorter exposure of the same blot to get a non-saturated picture of the 110 kDa bands. All hairpins reduced the expression of NRG1 isoforms, with hp1 and 2 being most efficient. B. Left: TPLSM images of HEK293 cells transfected, respectively, with the following constructs: 1. control group: tomato dsRed (as a cellular marker), SEP-NRG1 type I, and a non-relevant control hairpin; 2. hp1 group: tomato dsRed, SEP-NRG1 type I, and hp1; 3. hp2 group: tomato dsRed, SEP-NRG1 type I, and hp2; 4. hp3 group: tomato dsRed, SEP-NRG1 type I, and hp3. Right: same as that in the left, except that SEP-NRG1 type III was transfected instead of type I. C. Quantification of the expression level of SEP-NRG1 type I for different groups. The relative expression level of SEP-NRG1 type I was quantified as the green fluorescence (SEP-NRG1 type I) to red fluorescence (tomato dsRed) ratio (control: 1.5 ± 0.33 , $n=79$

cells; hp1: 0.31 ± 0.24 , n=52 cells; hp2: 0.18 ± 0.14 , n=46 cells; hp3: 0.28 ± 0.07 , n=67 cells; $P < 0.01$ control compared to all other groups). D. same as that in C, except the expression level of SEP-NRG1-type III was quantified instead of type I (control: 0.42 ± 0.05 , n=95 cells; hp1: 0.09 ± 0.01 , n=73 cells; hp2: 0.09 ± 0.02 , n=53 cells; hp3: 0.13 ± 0.02 , n=58 cells; $P < 0.01$ control compared to all other groups). All three hairpin constructs significantly suppressed the expression of both SEP-NRG1 type I and type III. E. Quantification of the EPSCs recorded from paired un-infected (control) and infected cells in CA1 region. CA1 cells were infected with a lenti virus expressing erbB4 hp2. CA3 cells were infected with a high titer virus expressing NRG1 hp1 (as in Fig. 6), together with another high titer virus expressing a NRG1 type III construct with silent mutations that avoid hp1 targeting. Co-expression of NRG1 and hp1 can be visualized since NRG1 type III was labeled with SEP (green), and the hp1 virus expressed tDimer (red). This rescued the phenotype of only expressing erbB4 hp2 in CA1 neurons (AMPA: control 1 ± 0.11 ; infected: 0.6 ± 0.18 , n=7 pairs, $P < 0.05$; NMDAR: control 1 ± 0.27 ; infected 0.6 ± 0.22 , n=7 pairs, $P < 0.05$).

References:

- Huang, Y. Z., Won, S., Ali, D. W., Wang, Q., Tanowitz, M., Du, Q. S., Pelkey, K. A., Yang, D. J., Xiong, W. C., Salter, M. W., and Mei, L. (2000). Regulation of neuregulin signaling by PSD-95 interacting with ErbB4 at CNS synapses. *Neuron* 26, 443-455.
- Kopeck, C. D., Li, B., Wei, W., Boehm, J., and Malinow, R. (2006). Glutamate receptor exocytosis and spine enlargement during chemically induced long-term potentiation. *J Neurosci* 26, 2000-2009.
- Li, B., Otsu, Y., Murphy, T. H., and Raymond, L. A. (2003). Developmental decrease in NMDA receptor desensitization associated with shift to synapse and interaction with postsynaptic density-95. *J Neurosci* 23, 11244-11254.
- Wang, J. Y., Miller, S. J., and Falls, D. L. (2001). The N-terminal region of neuregulin isoforms determines the accumulation of cell surface and released neuregulin ectodomain. *J Biol Chem* 276, 2841-2851.

Supplemental Figure 1



Supplemental Figure 2

